The Company of Biologists

RETRACTION

Retraction: Suppression of intestinal tumorigenesis in *Apc* mutant mice upon Musashi-1 deletion. J. Cell Sci. doi: 10.1242/jcs.197574

Andy R. Wolfe, Amanda Ernlund, William McGuinness, Carl Lehmann, Kaitlyn Carl, Nicole Balmaceda and Kristi L. Neufeld

The journal is retracting 'Suppression of intestinal tumorigenesis in *Apc* mutant mice upon Musashi-1 deletion' by Andy R. Wolfe, Amanda Ernlund, William McGuinness, Carl Lehmann, Kaitlyn Carl, Nicole Balmaceda and Kristi L. Neufeld (2017). *J. Cell Sci.* **130**, 805-813 (doi: 10.1242/jcs.197574).

This notice updates and replaces the Expression of Concern (doi: 10.1242/jcs.210690) relating to the above-referenced article.

After concerns were raised by a reader, Journal of Cell Science detected the following issues with the data in the above article:

  1) The actin loading control in the +/+ lane of the distal sample in Fig. 2A is identical to the actin loading control in the –/– lane of the proximal sample in Fig. 3A.

  2) Both actin loading controls in the proximal sample in Fig. 2B are identical to the actin loading controls in the medial sample in Fig. 3A.

The journal contacted Dr Kristi Neufeld, the corresponding author, who in accordance with institutional policy, referred the issue to the Research Integrity Officer. The journal also contacted the Director of Research Integrity at the University of Kansas.

In consultation with the Director of Research Integrity at The University of Kansas, Dr Neufeld then provided the following statement:

"This article has been withdrawn by the authors. After notification of inconsistencies in some of the figure panels, the senior author found that Fig. 2A, Fig. 2B and Fig. 3A were not consistent with the primary data. Due to this concern and the length of time required to repeat the experiments in question, the authors wish to retract the paper. We sincerely regret this situation and extend our deepest apologies to the scientific community."

The authors have agreed to this retraction.

PUBLISHER'S NOTE

Expression of Concern: Suppression of intestinal tumorigenesis in *Apc* mutant mice upon Musashi-1 deletion. Andy R. Wolfe, Amanda Ernlund, William McGuinness, Carl Lehmann, Kaitlyn Carl, Nicole Balmaceda, Kristi L. Neufeld. J. Cell Sci. doi: 10.1242/jcs.197574

Michael Way
Editor-in-Chief, Journal of Cell Science (jcs@biologists.com)

This Expression of Concern relates to the article 'Suppression of intestinal tumorigenesis in *Apc* mutant mice upon Musashi-1 deletion' by Andy R. Wolfe, Amanda Ernlund, William McGuinness, Carl Lehmann, Kaitlyn Carl, Nicole Balmaceda and Kristi L. Neufeld. J. Cell Sci. 2017 **130**, 805-813 (doi: 10.1242/jcs.197574).

We have recently been made aware of concerns regarding some of the data in Fig. 2A and B, and Fig. 3A. After discussion with the corresponding author, Kristi Neufeld, this matter has been referred to the authors' institute. Journal of Cell Science is publishing this Note to make readers aware of the issue, and we will provide further information once it has been resolved.

This course of action follows the advice set out by COPE (Committee on Publication Ethics), of which Journal of Cell Science is a member.

The Company of **Biologists**

RESEARCH ARTICLE

Suppression of intestinal tumorigenesis in *Apc* mutant mice upon Musashi-1 deletion

Andy R. Wolfe, Amanda Ernlund, William McGuinness, Carl Lehmann, Kaitlyn Cart, Nicole Almaceda and Kristi L. Neufeld*

ABSTRACT

Therapeutic strategies based on a specific oncogenic target are better justified when elimination of that particular oncogene reduces tumorigenesis in a model organism. One such oncogene, Musashi-1 (*Msi-1*), regulates translation of target mRNAs and is implicated in promoting tumorigenesis in the colon and other tissues. Msi-1 targets include the tumor suppressor adenomatous polyposis coli (*Apc*), a Wnt pathway antagonist lost in ~80% of all colorectal cancers. Cell culture experiments have established that *Msi-1* is a Wnt target, thus positioning Msi-1 and Apc as mutual antagonists in a mutually repressive feedback loop. Here, we report that intestines from mice lacking Msi-1 display aberrant Apc and Msi-1 mutually repressive feedback, reduced Wnt and Notch signaling, decreased proliferation, and changes in stem cell populations, features predicted to suppress tumorigenesis. Indeed, mice with germline *Apc* mutations (*Apc^Min*) or with the *Apc*^1322T truncation mutation have a dramatic reduction in intestinal polyp number when *Msi-1* is deleted. Taken together, results provide genetic evidence that Msi-1 contributes to intestinal tumorigenesis driven by Apc loss, and validate the pursuit of Msi-1 inhibitors as chemo-prevention agents to reduce tumor burden.

KEY WORDS: Musashi-1, Msi-1, Adenomatous polyposis coli, Apc, Intestinal tumorigenesis, Wnt, Notch

INTRODUCTION

Mutation of the tumor suppressor adenomatous polyposis coli (*APC*) is considered an initiating event in over 80% of all colon cancers (Vogelstein et al., 1989). APC is best characterized as a negative regulator of the canonical Wnt pathway. As such, APC acts as a scaffold for a complex that marks the transcription factor β-catenin for proteasomal degradation. Wnt signaling is important in the maintenance of the intestinal stem cell niche. Conditional loss of *Apc* in intestines of adult mice leads to an increased size of the progenitor population, with more proliferative and undifferentiated cells (Sansom et al., 2004). When *Apc* is conditionally deleted in intestines of adult mice, one of the most highly upregulated transcripts encodes the RNA-binding protein Musashi-1 (Msi-1) (Sansom et al., 2004). Intestinal polyps in mice with germline *Apc* mutations (*Apc^Min*) also show an upregulation of Msi-1 (Potten et al., 2003) and *Msi-1* has been identified as a Wnt target gene (Rezza et al., 2010; Spears and Neufeld, 2011).

Department of Molecular Biosciences, University of Kansas, 7049 Haworth Hall, 1200 Sunnyside Avenue, Lawrence, KS 66045, USA.

*Author for correspondence (klneuf@ku.edu)

C.L., 0000-0003-2205-4195; K.C., 0000-0001-6197-4173; N.B., 0000-0002-9670-5907; K.L.N., 0000-0003-3653-9385

Msi-1 is an RNA-binding protein that was originally identified in *Drosophila* as an essential regulator of asymmetric cell division in sensory organ precursor cells (Nakamura et al., 1994). Msi-1 is also expressed in mouse neuronal stem cells and is used as a marker of stem and transit-amplifying cells in the large and small intestines (Nishimura et al., 2003; Potten et al., 2003). Msi-1 binds to the 3′ untranslated region (UTR) of target mRNAs and blocks translation by competing with translation initiation factor eIF4G for interaction with poly(A)-binding protein (Kawahara et al., 2008). The first identified Msi-1 target mRNA was *Numb*, a negative regulator of Notch (Imai et al., 2001). Further research has revealed many potential Msi-1 targets. One study identified 64 Msi-1-bound mRNAs, many of which are associated with cell proliferation, differentiation, cell cycle and apoptosis (de Sousa Abreu et al., 2009). Cross-linking immunoprecipitation followed by high-throughput sequencing (CLIP-Seq) analysis of mouse intestinal epithelial cells revealed over 2200 potential Msi-1 targets (Li et al., 2015). Many human colorectal tumors display a significant increase in Msi-1 mRNA and protein compared to adjacent normal tissue (Sureban et al., 2008; Smith et al., 2015). Msi-1 overexpression can transform rat intestinal epithelial cells (Rezza et al., 2010) and Msi-1 knockdown in human colon cancer cells leads to retardation of tumor growth in a xenograft model (Sureban et al., 2008). Similar opposing phenotypes for Msi-1 gain and loss of function were also seen for mammary and brain cells (Rezza et al., 2010; Muto et al., 2012). Taken together, these data implicate Msi-1 in growth regulation of cell lines; however, until recently, little has been understood about the role of Msi-1 in intestinal tissue.

Our previous work revealed a mutually repressive feedback loop between Apc and Msi-1 in cultured cells (Spears and Neufeld, 2011). As a negative regulator in the Wnt signaling pathway, Apc inhibits *Msi-1* transcription (Rezza et al., 2010; Spears and Neufeld, 2011). Conversely, Msi-1 binds to *Apc* mRNA and blocks translation (Spears and Neufeld, 2011). Although *in vitro* evidence supports an integral role for the Apc and Msi-1 negative-feedback loop in gene regulation, the existence of this Apc and Msi-1 antagonistic relationship in intestinal tissue is unknown. Further, the consequences of disrupting this mutually repressive feedback loop in an intestinal tumor model have yet to be determined. Here, we investigate the role of Msi-1 in intestinal tumorigenesis by eliminating Msi-1 in a classic mouse model of intestinal cancer, *Apc^Min*, and also in a mouse model with an *Apc* mutation that closely resembles alterations in human colon cancer, *Apc*^1322T (Pollard, et al., 2009). Our results provide evidence for an Apc and Msi-1 double negative feedback loop in the mouse intestine and support a key role for Msi-1 in intestinal tumorigenesis. Furthermore, our results reveal several consequences of Msi-1 loss that might contribute to intestinal polyp reduction in mice lacking Msi-1. Taken together, our findings support the pursuit of Msi-1 inhibitors as potential chemo-prevention or therapeutic agents.

RESULTS

Msi-1$^{-/-}$ mice show proliferation defects in the small intestine

To understand the role of Msi-1 in intestinal homeostasis, we investigated the intestinal phenotype in mice homozygous for an *Msi-1* deletion (Fig. S1). Because mice completely lacking Msi-1 have greatly reduced viability when in the C57BL/6 background (Sakakibara et al., 2002), experiments with the Msi-1-null allele were performed in mice of the outbred stock CD-1, which show no such viability reduction. There was not a significant difference in total body, spleen and liver weight, or in colon length between wild-type mice and age-matched mice lacking Msi-1 (Fig. 1A–D). However, Msi-1-null mice had small intestines that were significantly shorter than those of their wild-type counterparts (Fig. 1D). Consistent with the shorter small intestines observed in the Msi-1-null mice, each of the three sections of the small intestine displayed a significant reduction in epithelial cell proliferation as assessed by determining the percentage of crypt cells that were positive for Ki-67 (Fig. 1E).
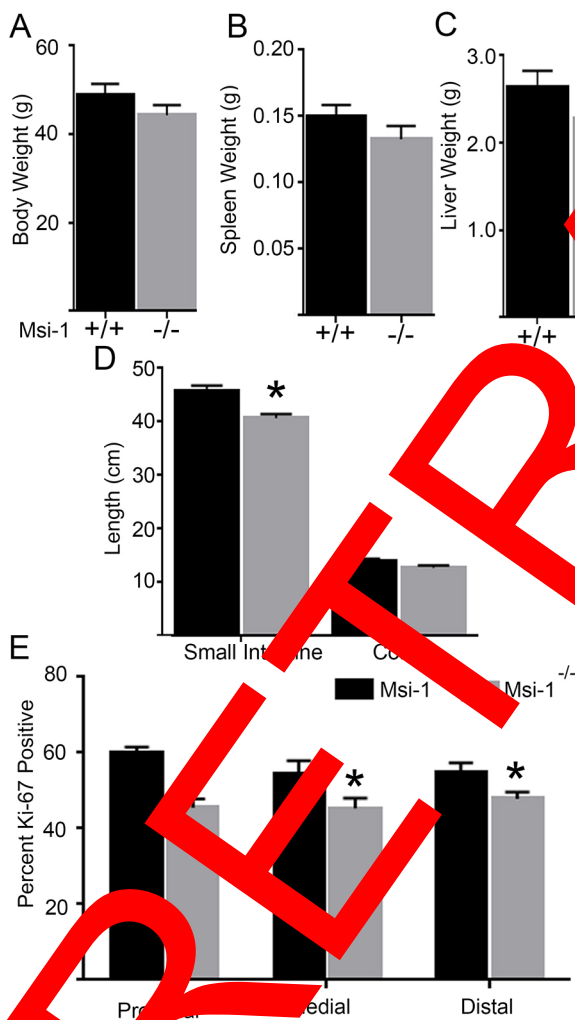

Fig. 1. *Msi-1$^{-/-}$ mice have shorter small intestines and reduced proliferation.* *Msi-1$^{+/+}$* and *Msi-1$^{-/-}$* mice were killed at 12 weeks of age. Body weight (A) as well as small intestine and colon length (B) were measured (*n*=16 per genotype). (C) Ki-67-positive cells were scored in ≥20 crypts for each of three small intestinal sections in at least eight mice of each genotype. Graphs represent mean±s.e.m. *P<0.05 (two-tailed *t*-test).

Small intestines from Msi-1$^{-/-}$ mice display reduced Wnt and Notch signaling

We focused our subsequent investigation on the small intestine, where tissue shortening and reduced proliferation in mice lacking Msi-1 was more dramatic compared with in the colon. Initially, we examined the Apc and Msi-1 mutually repressive feedback loop, previously identified and characterized in cultured cells (Spears and Neufeld, 2011) (Fig. S2). Consistent with our *in vitro* results and in support of a mutually repressive feedback loop, we observed higher levels of Apc protein in Msi-1-null mice compared to wild-type mice (Fig. 2A). As would be expected to accompany higher levels of Apc, we also observed a decrease in β-catenin protein levels in Msi-1-null mice (Fig. 2B). Furthermore, Msi-1-null mice displayed lower levels of Wnt target genes *Myc*, *Axin2*, *Lgr5*, and cyclin D1 (*Ccnd1*) mRNA than their wild-type counterparts (Fig. 2C–F). The exception to this was with the distal tissues where *Lgr5* and cyclin D1 mRNA levels were higher in Msi-1-null mice than in wild-type mice.

The Notch signaling pathway is negatively regulated by another established Msi-1 target, Numb. Numb protein levels were higher in intestines from Msi-1-null mice than from wild-type mice (Fig. 3A). Moreover, in intestines from Msi-1-null mice, we saw a decrease in *Hes1* mRNA, a direct Notch target, and an increase in *Math1* (also known as *Atoh1*) mRNA, which is indirectly repressed by Notch signaling (Fig. 3B,C). Taken together, these results indicate that mice lacking Msi-1 show signs of reduced Wnt and Notch signaling.

Msi-1$^{-/-}$ mice show stem cell alterations

The intestine is maintained by two stem cell populations. Actively cycling crypt base columnar (CBC) stem cells are located at the crypt bottom and express Lgr5 (Barker et al., 2007). Quiescent stem cells are located at a position '+4' relative to the crypt base and express markers including Dclk-1 (Potten et al., 2003; Giannakis et al., 2006; Barker et al., 2007; Gagliardi et al., 2012). Msi-1 is expressed within both stem cell populations and has been referenced as a stem cell marker (Kayahara et al., 2003; Potten et al., 2003; Munoz et al., 2012). We examined both active and quiescent stem cell populations for their response to loss of Msi-1.

We explored the quiescent +4 stem cell population using Dclk-1 as a marker (Fig. 4D). Only positive cells in the crypt were scored in order to distinguish quiescent stem cells from the Dclk-1-positive differentiated Tuft cells, which reside in or near the villus (May et al., 2008; Gerbe et al., 2009; Gagliardi et al., 2012). Unexpectedly, mice lacking Msi-1 showed higher numbers of Dclk-1-positive cells in all three sections of the small intestine when compared to wild-type mice (Fig. 4A).

As an initial analysis of the CBC stem cell population, we used an *ex vivo* system to culture isolated small intestinal crypts from the mice. In this system, adapted from Sato et al. (2009), crypts are removed from surrounding mesenchymal tissue, separated from villi and grown in a three-dimensional (3D) matrix with exogenous components that enhance Wnt signaling (Ootani et al., 2009). Cultured crypts produce organoid structures, with differentiated secretory and absorptive cells present along the luminal surface. After 24 h in culture, the organoids will produce new crypt-like protrusions from stem cells (Sato et al., 2009). We used these protrusions as a marker of 'stemness'.

To provide proof of concept that this *ex vivo* culture system could be used to assess stem cell population differences, we first compared cultured crypts isolated from an *Apc*$^{1322T/+}$ mouse and a wild-type mouse. A previous study using the *Apc*$^{1322T/+}$ mouse model showed that these mice have more Lgr5-positive 'active' stem cells than wild-type mice (Lewis et al., 2010). After culturing organoids for
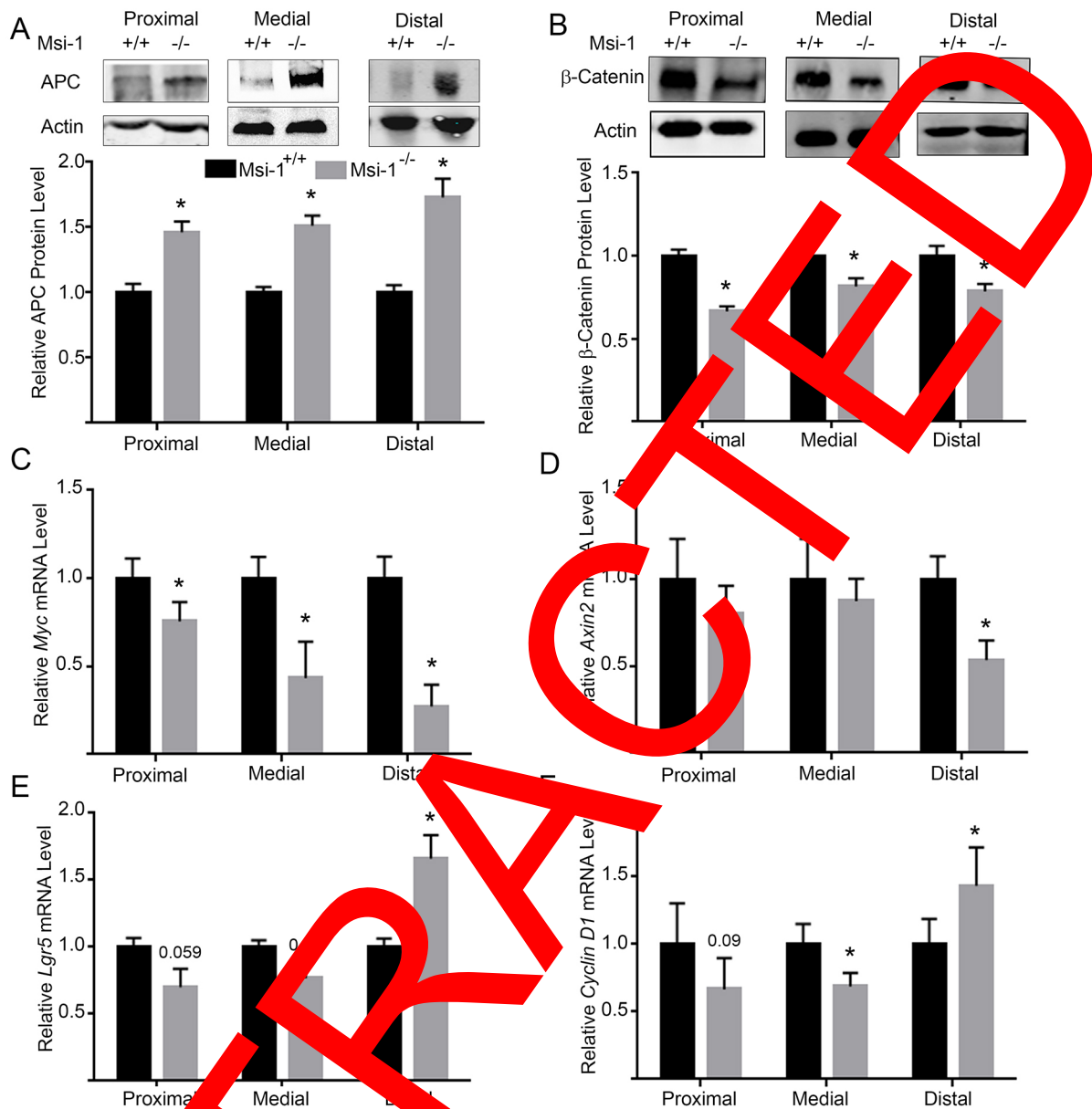
Fig. 2. Msi-1$^{-/-}$ mice display decreased Wnt activity in small intestinal epithelia. Proteins and RNAs were extracted from epithelial cells isolated from the three regions of the small intestines of Msi-1$^{+/+}$ and Msi-1$^{-/-}$ mice. (A,B) Protein samples from ten mice of each genotype were probed for APC and β-catenin (representative blots in A and B, respectively). Lower panels display average band intensities normalized to actin loading control and relative to Msi-1$^{+/+}$ mouse samples. (C–F) Total RNA was analyzed for levels of the downstream Wnt signaling targets Myc (C), Axin 2 (D), Lgr5 (E) and cyclin D1 (F). n=16 per genotype. Graphs represent mean±s.e.m. *P<0.05 (two-tailed t-test).

5 days, those from Apc^{1322T} mice had significantly more protrusions than organoids from wild-type mice (see Fig. 4E, as an example, and Fig. 4B).

Because Msi-1 overexpression was previously correlated with expansion of stem cell populations (Rezza et al., 2010), we expected that knockout of Msi-1 would result in organoids with fewer protrusions. Indeed, after 8 days of growth ex vivo, crypts from Msi-1-null mice had fewer protrusions per organoid than those from wild-type mice. Beginning at day nine, organoids were obscured from vision by debris in the cultures. Organoids from Msi-1-null mice that were re-plated after mechanical dispersion showed the same decrease in protrusions compared to passaged organoids from wild-type mice (data not shown).

Results gathered employing organoid culture protrusions as a marker of stemness were validated by identifying active stem cells in

tissue using the marker Lgr5. Labeling Lgr5 mRNA in tissue sections allowed us to directly score the CBC stem cells (Fig. 4F). We observed that the majority of crypts in mice lacking Msi-1 had only one or two Lgr5-positive cells (Fig. 4G). In mice with wild-type Msi-1, there was a significant shift in this distribution toward crypts displaying four and even five Lgr5-positive cells. These data are consistent with the organoid culture data and indicate that mice lacking Msi-1 are compromised for Lgr5-positive active stem cells in the small intestine.

Msi-1 promotes polyps in Apc mutant mouse models

Our studies indicated that small intestines from Msi-1-null mice were defective in Wnt and Notch signaling and had decreased proliferation and altered stem cell numbers. These findings, combined with previous in vitro studies supporting a role for Msi-

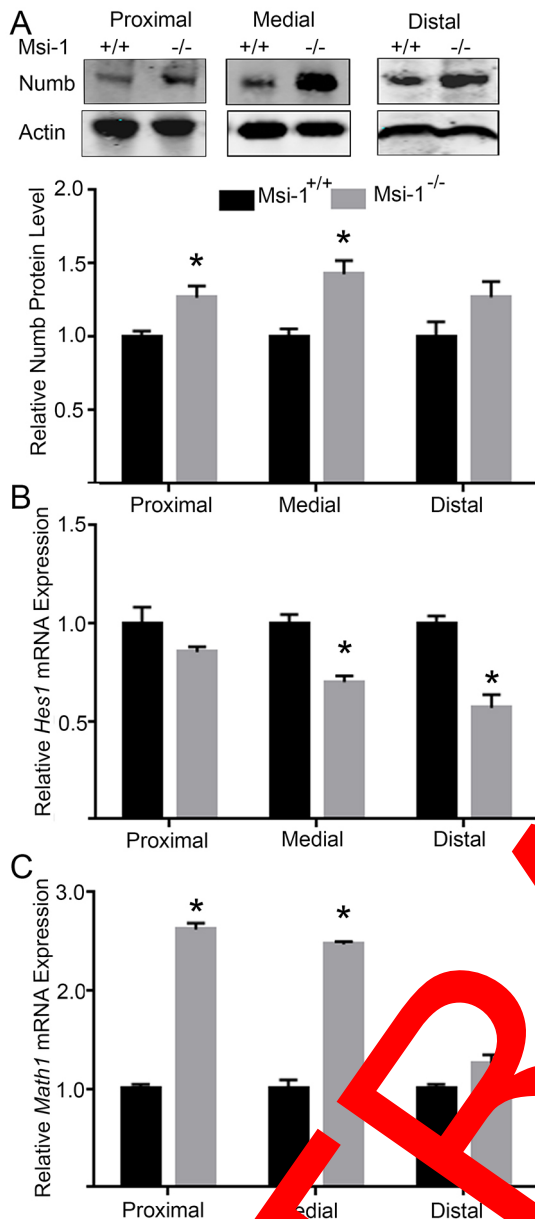**Fig. 3. *Msi-1*$^{-/-}$ mice display increased Notch activity in small intestinal epithelia.** Proteins and RNAs were extracted from epithelial cells isolated from the three regions of the small intestines of *Msi-1*$^{+/+}$ and *Msi-1*$^{-/-}$ mice. (A) Protein samples from ten mice of each genotype were probed for the Notch inhibitor Numb (a representative blot is shown). The lower panel displays average band intensities normalized to the actin loading control and relative to *Msi-1*$^{+/+}$ mouse samples. (B,C) Total RNA was analyzed for levels of the downstream Notch target *Hes1* (B) and a transcript repressed by Hes1, *Math1* (C). *n*, number per genotype. Graphs represent mean±s.e.m. *P<0.05 (two-tailed *t*-test).

1 in tumorigenesis (Sureban et al., 2008; Rezza et al., 2010), led to the hypothesis that Msi-1 plays a crucial role in tumorigenesis. To genetically test whether Msi-1 is involved in polyp formation, we introduced *Msi-1* mutations into mice with germline *Apc* mutations (*Apc*^{Min} or *Apc*^{1322T} mice were bred with CD-1 mice for seven generations to produce mice that were predominantly CD-1 (Fig. 5A). A total of 28 mice with the *Apc*^{Min} allele and null for *Msi-1* were analyzed and compared to 38 littermates with the *Apc*^{Min} allele but wild-type for Msi-1. By the age of 16 weeks, CD-1 *Apc*^{Min} mice developed 12 intestinal polyps on average. Elimination of

Msi-1 in these mice led to an ~80% reduction in polyp number with an average of 2.4 polyps per mouse (P<0.05; Fig. 5B,C, Table 1). Moreover, over a quarter of the *Apc*^{Min} mice lacking Msi-1 had no polyps (Fig. 5C, incidence). Although *Apc*^{Min} mice are a well-utilized model of inherited intestinal tumor susceptibility, the truncated Apc protein produced in these mice is shorter than Apc truncations typically associated with human colorectal cancer (Lamlum et al., 1999). *Apc*^{1322T} mice, on the other hand, carry a truncating *Apc* mutation at codon 1322, within the 'mutation cluster region' as defined from human CRC data (Pollard et al., 2009). To further explore the requirement for Msi-1 in tumorigenesis and confirm that the tumor phenotype is not specific to the model, *Apc*^{1322T} mice were bred with CD-1 mice for eight generations to produce mice that were predominantly CD-1 (Fig. 5D). We observed similar phenotypes in the *Apc*^{1322T} and *Apc*^{Min} mice. CD-1 *Apc*^{1322T} mice developed an average of 14 intestinal polyps by the age of 16 weeks. *Msi-1*-null *Apc*^{1322T} mice displayed a significant reduction in polyp number, with an average of five polyps per mouse (Fig. 5F). Moreover, there was a significant decrease in polyp incidence in mice without Msi-1; nearly all *Apc*^{1322T} mice with wild-type Msi-1 developed polyps and only 82% of *Apc*^{1322T} mice lacking Msi-1 developed polyps (Fig. 5F). Taken together, these data demonstrate that Msi-1 loss decreases polyposis, supporting an oncogenic role for Msi-1.

Looking at polyp distribution, we found a significant decrease in polyp incidence in all three sections of small intestine of *Apc*^{Min} mice lacking Msi-1 (Fig. 5G). Polyp numbers within each small intestinal region were also significantly decreased in *Apc*^{Min} mice lacking Msi-1 (Fig. 5H). Polyps within the proximal small intestine region of the Msi-1-null *Apc*^{Min} mice were significantly smaller than in *Apc*^{Min} mice with wild-type Msi-1 (Fig. 5I). There were so few polyps in the medial and distal small intestines of the Msi-1-null *Apc*^{Min} mice that a statistical comparison of their size was not possible. Similar to the *Apc*^{Min} mice, *Apc*^{1322T} mice lacking Msi-1 showed a decrease in polyp incidence in each of the intestinal sections, reaching significance in the proximal small intestine and colon (Fig. 5J). *Apc*^{1322T} mice lacking Msi-1 also exhibited a significant decrease in polyp number in all sections of the small intestine and colon (Fig. 5K). Finally, we observed a significant reduction in polyp size in the colons of *Apc*^{1322T} mice lacking Msi-1 (Fig. 5L). Taken together, this polyp analysis supports a role for Msi-1 in promoting *Apc* mutation-driven tumorigenesis throughout the intestine.

DISCUSSION

Msi-1 protein and mRNA levels were elevated in tissue from some colorectal tumors when compared to adjacent normal tissue (Sureban et al., 2008; Smith et al., 2015). Overexpression of Msi-1 in cultured normal intestinal epithelial cells resulted in tumor formation in nude mouse xenografts (Sureban et al., 2008). Conversely, knockdown of Msi-1 levels in human colon cancer cells slowed tumor growth in a similar xenograft model (Rezza et al., 2010). Taken together, these results have spurred interest in pursuing Msi-1 as a potential therapeutic target for colorectal and other cancers. To this end, we previously reported that treatment of colon cancer cells with a novel Msi-1 inhibitor slowed cell growth (Lan et al., 2015). Here, using two mouse models where intestinal tumors are initiated by different germline *Apc* mutations, we provide proof of concept that Msi-1 loss results in a dramatic decrease in tumorigenesis (Fig. 5, Table 1). We report a significant decrease in tumor incidence, with 12–28% of the Apc mutant Msi-1-null mice remaining tumor-free by the end of the 16 week study. Moreover,
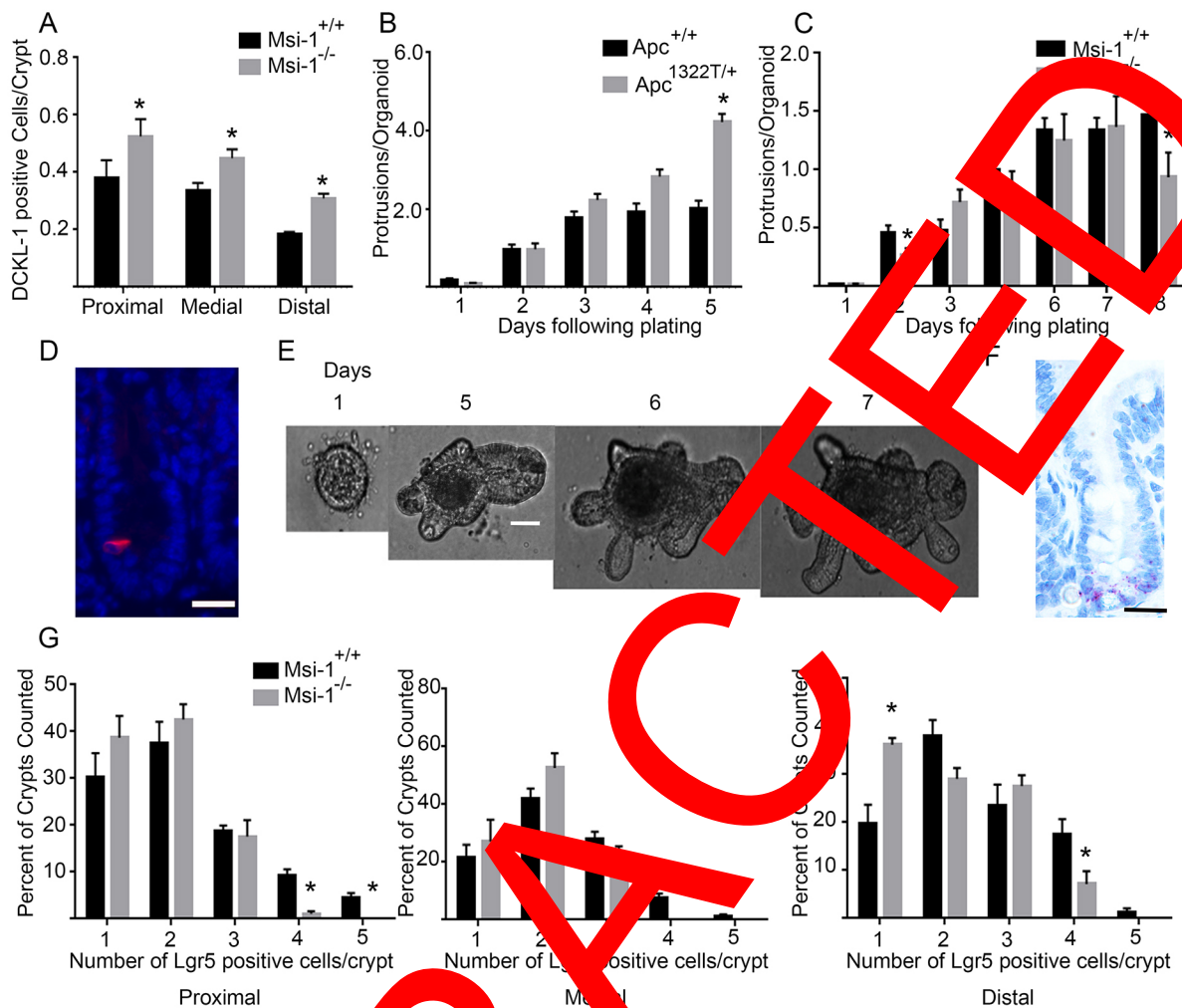
Fig. 4. Msi-1 alters stem cell number. (A) DCLK-1 positive quiescent stem cells were scored by counting ≥20 crypts in at least eight mice of each genotype. (B) *Ex vivo* cultures of small intestine crypts from *Apc*[1322T] mice proceeded so far except that organoid cell protrusions (E) could serve as a surrogate measurement for active stem cells. (C) Organoid cell protrusions from *Msi-1*^{+/+} and *Msi-1*^{−/−} mice. (D) Numbers of *Lgr5*-positive cells per crypt in *Msi-1*^{+/+} and *Msi-1*^{−/−} mice assessed following *in situ* hybridization. Data from at least 20 crypts scored for at least eight mice per genotype are represented as the percentage of the crypts scored containing one to five *Lgr5*-positive cells. Examples from each technique are shown: (D) DCLK-1 staining; (E) intestine crypt organoid from *Apc*[1322T] mice various time points after initial plating; (F) *Lgr5 in situ* hybridization. Graphs represent mean±s.e.m. *P<0.05 (two-tailed *t*-test). Scale bars: 25 µm (D,F); 100 µm (E).

the Msi-1-deficient mice that did display tumors displayed a ∼53–75% reduction in tumor number compared to their wild-type counterparts.

In the small intestines of both Apc models, we observed an uneven polyp distribution, with more polyps occurring in the proximal section and progressively fewer moving toward the distal portion. Regional differences were also observed in the levels of Wnt and Notch pathway component proteins and mRNA (Figs 2 and 3). These differences include higher than normal levels of cyclin D1 and *Lgr5* in the distal portions of Msi-1-null small intestines compared to normal, but lower levels in all other regions (Fig. 2E). Regional differences in gene expression patterns in the pig small intestine have been reported (Mach et al., 2014), and our data support the concept that different small intestine sections have distinct properties that may contribute to varying sensitivity to Msi-1 loss and tumorigenesis.

Our demonstration that overall Wnt and Notch signaling are diminished in mice lacking Msi-1 identifies these signaling pathways as potential contributors to enhanced tumorigenicity mediated by Msi-1. Based on results from studies performed using human colon cancer cell lines, we previously proposed a model

describing Apc and Msi-1 in a mutually repressive feedback loop (Spears and Neufeld, 2011). As predicted by this model, small intestines from mice lacking Msi-1 displayed higher Apc levels, lower β-catenin levels and reduced levels of Wnt target gene transcripts compared to their wild-type littermates (Fig. 2). Small intestines from mice lacking Msi-1 also exhibited diminished cell proliferation, a reduced number of Lgr5-positive cells and fewer active stem cells when grown as organoids in 3D culture (Figs 1C and 4C,G, respectively). These changes in proliferation and stem cell number are consistent with the opposite phenotype reported for Msi-1 overexpressing mice (Cambuli et al., 2015; Li et al., 2015). Although the Msi-1 overexpressing mice did not display changes in Wnt target gene RNA levels, *Apc* mRNA co-purified with Msi-1 isolated from these mice (Li et al., 2015). The expected consequence of elevated Apc and reduced β-catenin levels, reduced Wnt target gene expression and proliferation, in mice lacking Msi-1 is a reduction in the opportunity for loss of heterozygosity at the *Apc* locus, which is typically required for tumor initiation. Moreover, the Notch signaling pathway is predicted to contribute to this phenotype by modulating proliferation and differentiation of cells near the crypt base
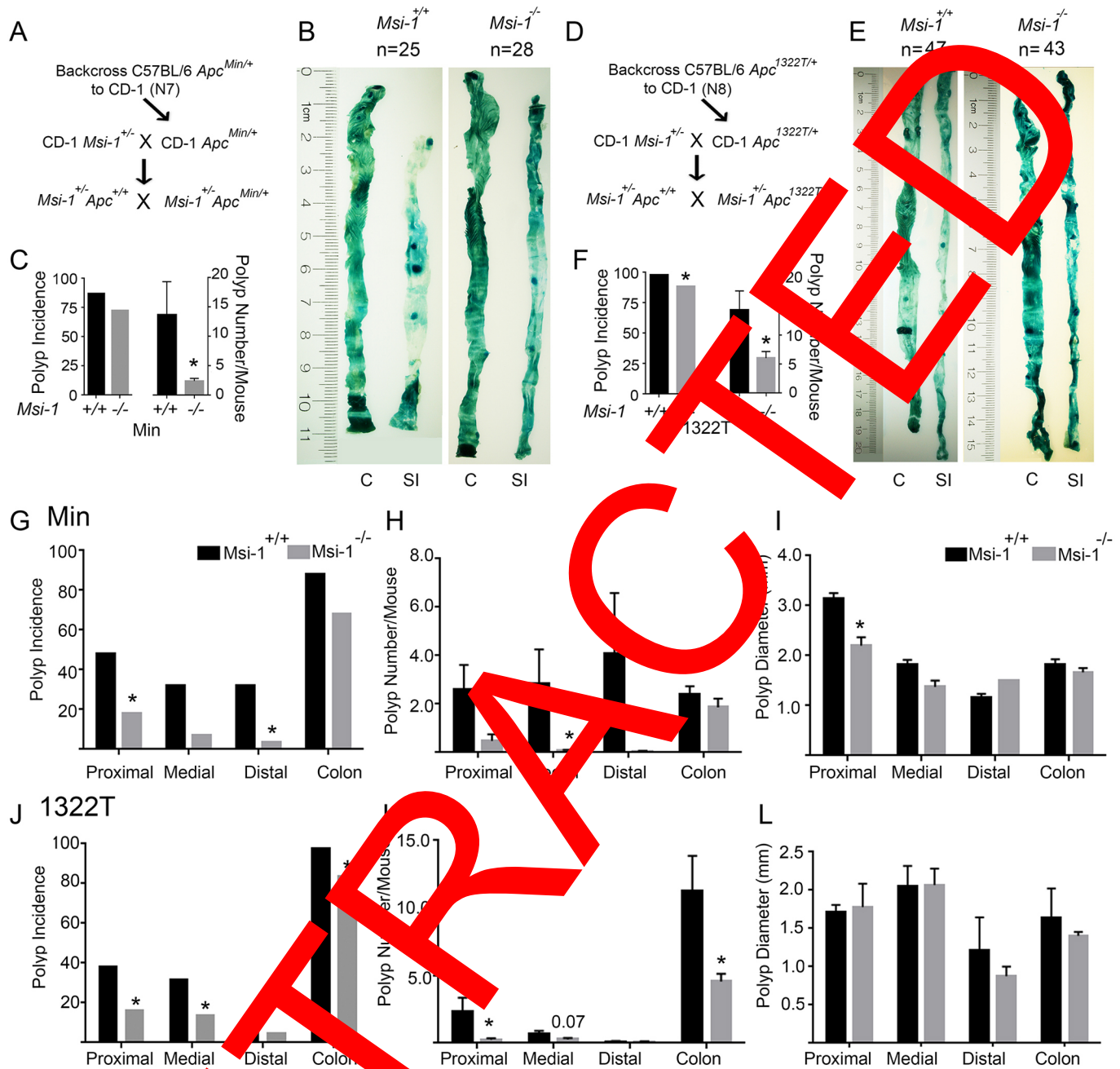
Fig. 5. Msi-1 promotes polyp formation in *Apc* mutant mice. (A) C57Bl6 *Apc^Min/+* mice were backcrossed for seven generations with CD-1 mice. These N7 mice were bred with *Msi-1^−/−* mice to obtain *Apc^Min/+ Msi-1^−/−* and *Apc^Min/+ Msi-1^+/+* mice. (B) Representative images of the colon and proximal small intestines with polyps. The *Apc^Min/+ Msi-1^−/−* mice (n=28) have a lower incidence of polyp formation and fewer formed polyps than *Apc^Min/+ Msi-1^+/+* mice (n=38). (D) C57Bl6 *Apc^1322T/+* were backcrossed for eight generations with CD-1 mice. These mice were further bred to *Msi-1^−/−* mice to obtain *Apc^1322T/+ Msi-1^−/−* and *Apc^1322T/+ Msi-1^+/+* phenotypes. (F) Representative images of the colon and proximal small intestines with polyps. (F) *Apc^1322T/+ Msi-1^−/−* (n=46) have a lower incidence of polyp formation and fewer formed polyps than *Apc^1322T/+ Msi-1^+/+* (n=57). (G) *Apc^Min/+ Msi-1^−/−* mice show lower polyp incidence in all intestinal regions. *Apc^Min/+ Msi-1^−/−* mice have fewer polyps in all regions (H) and smaller polyps in the proximal small intestine and colon (I). (J) *Apc^1322T/+ Msi-1^−/−* mice show lower polyp incidence in all intestinal regions. *Apc^1322T/+ Msi-1^−/−* mice have fewer polyps in all regions (K) and smaller polyps in the colon (L). Graphs represent the mean. *P<0.05 [Fisher's exact test (incidence) or *t*-test (polyp number and diameter)].

(Van Dussen et al., 2012). The potential for Msi-1 to modulate both Notch and Wnt signaling suggests a key role for Msi-1 in crypt cell homeostasis.

Continued renewal of the epithelial cells lining the intestine depends on stem cells located near the crypt base (Stappenbeck et al., 1998). Two types of stem cells exist: the actively cycling CBC stem cells and the quiescent '+4' stem cells. The +4 stem cells are required to maintain homeostasis within the intestinal crypts

(Sangiorgi and Capecchi, 2008). However, studies show that most of the characterized stem cell markers are expressed in a 'stem zone', and not exclusively in a single stem cell pool (Itzkovitz et al., 2012; Munoz et al., 2012). Of note, Msi-1 is reported to mark both stem cell populations in small intestine and colon (Kayahara et al., 2003; Potten et al., 2003; Munoz et al., 2012). Furthermore, Msi-1 is also expressed in a gradient within the two stem cell populations with the +4 cells having higher Msi-1 expression than the CBC cells

Table 1. Polyp data from *Apc* mutant mice

| | Apc^{1322T} | | | | Apc^{Min} | | | |
| | Polyp number | | Penetrance (%) | | Polyp number | | Penetrance (%) | |
	$Msi\text{-}1^{+/+}$	$Msi\text{-}1^{-/-}$	$Msi\text{-}1^{+/+}$	$Msi\text{-}1^{-/-}$	$Msi\text{-}1^{+/+}$	$Msi\text{-}1^{-/-}$	$Msi\text{-}1^{+/+}$	$Msi\text{-}1^{-/-}$
Proximal	2.35±1.00	0.26±0.10	38.30	16.28	2.61±1.29	0.48±0.?	39.13	7.24
Medial	0.70±0.20	0.26±0.11	31.91	13.95	2.83±1.83	0.07±0.05	21.74	6.90
Distal	0.14±0.07	0.07±0.05	6.38	4.65	4.08±3.21	0.03±0.03	36.09	3.45
Colon	11.15±2.58	5.12±0.92	97.87	83.72	2.39±0.45	1?±0.36	?	65.52
Total	14.36±3.29	5.70±1.04	97.87	88.37	11.91±5.80	?±0.43	86.?	72.4

Results are shown as mean±s.e.m. for Apc^{1322T} $Msi\text{-}1^{+/+}$ (n=25), Apc^{1322T} $Msi\text{-}1^{-/-}$ (n=28), Apc^{Min} $Msi\text{-}1^{+/+}$ (n=?), Apc^{Min} $Msi\text{-}1^{-/-}$ (n=43) mice.

(Maria Cambuli et al., 2013). Here, we provide evidence that mice lacking Msi-1 display an increase in quiescent +4 cells and a decrease in active CBC cells (Fig. 4). This result is consistent with the increase in mRNA for the CBC marker *Lgr5* and increased number of Lgr5-positive cells reported in mice that overexpress Msi-1 (Cambuli et al., 2015; Li et al., 2015). Taken together, these data indicate a role for Msi-1 in stem cell regulation. However, the opposing changes in the two stem cell populations point to a distinct role for Msi-1 within each population. Moreover, our finding of higher Lgr5 mRNA levels in the distal small intestine of Msi-1-knockout mice again raises the potential for varying roles of Msi-1, dependent on the intestinal region. There are reports that Msi-1 can inhibit or promote translation in a context-dependent manner (MacNicol et al., 2011; Takahashi et al., 2013). One potential mechanism for the differential role of Msi-1 in the two stem cell pools and the different intestinal regions is that features of the stem cell niche or intestinal region dictate whether Msi-1 blocks or promotes translation. In addition, the ability of Msi-1 to auto-regulate potentially contributes to the disparate roles for Msi-1 in these different populations (Arumugam et al., 2012). Recently published mouse models (Maria Cambuli et al., 2013; Cambuli et al., 2015) should help clarify the role of Msi-1 in different cell populations.

Our result that Msi-1 elimination leads to a reduction in polyp number in two different *Apc* mutant mouse lines contrasts with data from a study published during the preparation of this manuscript that showed that elimination of Msi-1 in Apc^{Min} mice does not result in decreased polyp formation (Li et al., 2015). Rather, a ∼50% reduction in polyp number was observed only when both Msi-1 and Msi-2 were eliminated (Li et al., 2015). Several key differences in the study design and the mouse models analyzed likely underlie these contradictory results and might provide further clues regarding oncogenic Msi-1 functions. First, the present study utilized germline *Msi-1*-knockout mice, while the other study induced Msi-1 loss in 6-week-old mice. Intestinal tumors are thought to initiate in Apc^{Min} mice within 2 weeks of birth (Shoemaker et al., 1995), well before the Msi-1 withdrawal at 6 weeks. Perhaps Msi-1 plays a key role in this initiation phase of tumorigenesis and, at later stages, Msi-1 and Msi-2 function redundantly to support sustained tumor growth. Second, mice used for the present study lack Msi-1 in every cell, whereas in the previous study Msi-1 was eliminated only in intestinal epithelial cells through use of a villin promoter-driven Cre recombinase. Possibly, Msi-1 tumor-promoting functions are cell non-cell-autonomous. For example, Msi-1 might have a crucial tumor-promoting role in the stroma. Third, the genetic background of the mice is different, with outbred CD-1 mice used for the present study and inbred C57Bl/6:129 mice used in the other study. Mice with different genetic backgrounds are expected to contain different genetic modifiers that could alter the polyp phenotype and mask or enhance the contribution of Msi-1. Fourth, in the present study, mice

were analyzed at 16 weeks of age at which time the Apc^{Min} mice each had an average of 12 intestinal tumors (Fig. 5C). In the other study, mice were analyzed at 6 months of age at which time Apc^{Min} mice each had, on average, 10 intestinal tumors. This difference in polyp number alone nicely illustrates the genetic modifying effects of various mouse strains (Zeineldin and Neufeld, 2013). Finally, the age and diet of mice also differed in the two studies.

Here, we report that mice lacking Msi-1 display fewer tumors, and thereby provide evidence that Msi-1 plays an important role in intestinal tumorigenesis. This study provides proof of principle for the design and use of Msi-1 inhibitors as potential chemo-prevention agents and also validates the use of *Apc* mutant mouse models to test Msi-1 inhibitors in tumor prevention. Finally, we provide evidence that Wnt and Notch signals are altered in Msi-1-knockout mice, suggesting that these pathways can be used as biomarkers in testing the effect of potential Msi-1 inhibitors in the small intestine.

MATERIALS AND METHODS

Mouse husbandry

Mice were maintained at the Animal Care Unit at the University of Kansas according to animal use statement number 137-02. The research complied with all relevant federal guidelines and institutional policies. Mice were maintained on a Harlan 2018 diet. The $Msi\text{-}1^{-/-}$ mice, ICR.129(B6)-Msi1<tm1Okn>/OknRbrc (No.RBRC04435), were provided by the RIKEN BRC through the National Bio-Resource Project of the MEXT, Japan (Sakakibara et al., 2002) (Fig. S1). $Msi\text{-}1^{-/-}$ mice were bred with CD-1 mice from Jackson Laboratories to maintain the colony. For mechanistic studies, $Msi\text{-}1^{+/-}$ mice were bred, and their progeny $Msi\text{-}1^{-/-}$ and $Msi\text{-}1^{+/+}$ littermates were killed at 12 weeks of age at which time their organs were harvested. $Apc^{Min/+}$ mice were purchased from Jackson Laboratories and bred with CD-1 mice for seven generations to produce mice that were genetically predominantly CD-1. $Apc^{1322T/+}$ mice, a generous gift from Ian Tomlinson (Wellcome Trust Centre for Human Genetics, Oxford University, UK), were bred with CD-1 mice for eight generations to produce mice that were predominantly CD-1. These *Apc* mutant mice in the CD-1 background were then bred with Msi-1$^{+/-}$ mice for two generations to compare $Msi\text{-}1^{-/-}$ and $Msi\text{-}1^{+/+}$ littermates, each with the mutant *Apc* allele (Fig. 5). Polyp analysis was performed on mice killed at 16 weeks of age by an individual that was blind to the genotype.

Analysis of gross and microscopic pathology, polyp measurement

The gross and cellular histology of intestinal tissues were examined in progeny from the bred N7 generation of mice ($Apc^{Min/+}$ $Msi\text{-}1^{+/+}$ and $Apc^{Min/+}$ $Msi\text{-}1^{-/-}$) and in progeny from the bred N8 generation of mice ($Apc^{1322T/+}$ $Msi\text{-}1^{+/+}$ and $Apc^{1322T/+}$ $Msi\text{-}1^{-/-}$) at 16 weeks of age. For each mouse, the gastrointestinal tract from the stomach to the anal canal was dissected, opened longitudinally and fixed in 10% buffered formalin. Using a dissecting microscope, an investigator blind to the genotype of the animal examined the intestinal luminal surface for polyps. Intestinal polyps were located and diameter was measured with the aid of a dissection microscope (MZ8; Leica, Richmond, IL) equipped with an eyepiece graticule and

calibrated to a 50-mm-scale stage micrometer with 0.1 and 0.01 mm graduation. Polyp incidence was determined by dividing the number of mice with a polyp by the total number of mice.

Isolation of mouse intestinal epithelial cells

Intestinal epithelial cells were isolated according to a published protocol with minor modifications (Zeineldin and Neufeld, 2012). Briefly, immediately after killing the mice, their distal 3 cm of small intestine was removed, opened length-wise and rinsed with cold phosphate-buffered saline (PBS). Tissue was incubated in 0.04% sodium hypochlorite for 15 min on ice and then rinsed in cold PBS. The small intestine was then incubated on ice for 15 min in a 15 ml conical tube containing an EDTA with dithiothreitol (DTT) solution (1.5–3 mM EDTA and 0.5 mM DTT in PBS). After replacing the EDTA and DTT solution with cold PBS, tubes were shaken forcefully for 10 s to release the epithelial cells from the underlying tissue. The intestinal tissue was removed and placed in a fresh 15 ml conical tube containing the EDTA and DTT solution, and the process was repeated two additional times. The released epithelial cells were collected by centrifugation at 700 g for 5 min at room temperature. Pellets of epithelia from all three rounds of extraction were resuspended in PBS with protease inhibitors, combined and then split into two equal samples. The small intestinal epithelial cells were then pelleted and one tube was used for RNA extraction and the other for western blot analysis as described below.

Western blotting

Cells were washed twice with ice-cold PBS and then lysed in protein sample buffer (2% w/v sodium dodecyl sulfate, 10% glycerol, 50 mM Tris-HCl pH 6.8 and 0.06 mg/ml Bromophenol Blue). Proteins were separated using SDS-PAGE and 4–20% polyacrylamide gels and blotted onto nitrocellulose. Antibodies used for protein detection were against the following proteins: APC [1:3000, M2-APC (Wang et al., 2009)], Msi-1 (1:2000, [...], Millipore, Boston, MA), Numb (1:1000, #2756 Cell Signal, Bever[...], MA), β-catenin (1:1000, 610153 BD Biosciences, East Rutherford, NJ) and [...]ctin (1:5000, A2228 Sigma). Images acquired with Odyssey IR imager (Li-[...], Lincoln, NE) were analyzed with Image Studio Lite v5.0 (Li-Cor, Linc[...] NE). Results shown are representative images from 10 [...]nt mice from each genotype with all results used to calculate the a[...]ge ba[...] intensity.

Real-time PCR

RNA isolated utilizing Trizol (Invitrogen) ac[...]ing to the [...] instructions was analyzed using quantitative real[...] PCR (q[...]T-PCR). First-strand cDNA was prepared from 0.5 μg R[...]A using [...]ts of M-MuLV reverse transcriptase and Random 6 pri[...] (New Engla[...] abs, Ipswich, MA). RNA levels were normalized to [...]e internal control H[...] PCR was performed utilizing DyNAmo HS [...] Green (Thermo Scie[...]ic) and analyzed with a DNA Engine Op[...]n 2 [...]al cycler (Bio-Rad, Hercules, CA). Data was processed using [...] ΔΔC(T) m[...]d. The average ΔC(T) was calculated for target cDNA relative to the housekee[...] gene Hgprt transcript while the ΔΔC(T) of targe[...] DNA was calculated rel[...] to the wild-type littermates. A Mann–Wh[...]y nonparametric test was performed with data from 16 different mice [...] each geno[...]pe to calculate P-values.

Immunofluorescence stainin[...]

Immunofluorescenc[...] ining [...] ormalin-fix[...] araffin tissue sections was performed as described p[...]sly (Zeineld[...] t al., 2012). Briefly, samples were incubated with blockin[...] ffer (5% [...]ormal goat serum, 1% bovine serum albu[...] old fish ski[...] at[...] and 0.1% Triton X-100) for 1 h at room te[...]erature. [...]mples were th[...] ncubated with primary antibodies dilute[...] he blockin[...] buffer at 4°C overnight, followed by three washes with PBS [...] r 5 min ea[...] incubated with secondary antibodies di[...] in blockin[...] ffer for 1 h followed by three washes in PBS. Coverslips were [...] ed [...] slides with Prolong Antifade with DAPI (Invitrogen). Antibodie[...] ed include: anti-Ki-67 (1:400, D3B5, Cell Signaling) and anti-DCLK-1 ([...] ab31704, Abcam, Cambridge, MA) antibodies, and goat anti-rabbit-IgG [...] jugated to Alexa Fluor 568 (1:1000, Molecular Probes, Grand Island, NY). Negative controls included incubation with secondary antibody alone. These negative controls resulted in only minimal signal. Tissues were visualized using a PlanNeofluor 40×1.3 NA oil objective on a Carl Zeiss Axiovert Microscope 135 (Jena, Germany).

Organoid culture

The small intestines from 5-week-old mic[...] each genotype [...] opened longitudinally, washed 3× with cold HBS[...] Ca^{2+} and Mg^{2+} free) a[...] cut into ~1 cm pieces. The pieces were placed in[...] mM EDTA in PBS an[...] llowed to incubate on ice for 20 min. EDTA solut[...] s removed an[...] ssue was washed with 50 ml of cold HBSS. [...] r the HBS[...] h, 25 ml o[...] ld HBSS was added to the tissue. Intestin[...] ieces were shake[...] 5 m[...] t 3 shakes/second to dissociate crypts an[...] l. Solution[...] containing [...] and villi were poured through 70 μm fil[...] to remo[...] villi. The solution was then centrifuged at 250 g fo[...] in to pel[...] crypts an[...] he supernatant was removed. Crypt pellets [...] resus[...] ed in 25[...] of basal medium [advanced DMEM-F[...] (Gibc[...] . 12634-01[...] 200 mM L-glutamine and 10 mM Hepes [...] 7.5]. Cryp[...] ions we[...] entrifuged at 200 g and most of the super[...] nt was removed, [...] [...] l in which the crypt pellet was resuspende[...] ing widebore pipettes, [...] of crypt solution was added to 40 μl of ba[...] me[...] in 5% BSA-coated microfuge tubes (crypts diluted 1:2). 80 μl [...] Matrigel [...] Matrigel basement membrane matrix growth factor reduced, cat. no. 35[...] was added to the crypt solution (crypts: Matrigel=1:1). 40 μl of the cry[...] Matrigel solution was plated in 24-well plate[...] ubated for 20 min at 3[...]°C with 5% CO$_2$ to allow Matrigel to so[...]y. Once solidified, 400 μl of overlay was added to each well and [...] ubated at 37°C with[...]% CO$_2$ for the duration of the experiment. Overlay [...]luded: 100 ng/ml [...]gin (Peprotech cat. no. 250-38), 10 ng/ml EGF [...]eprotech cat. no. PM[...]044), 500 ng/ml R-spondin1 (Sino Biological cat. [...]50316-M08H) and [...]icillin-streptomycin (Gibco cat. no. 15140-148) in ba[...] edium. Organ[...]s and protrusions were scored beginning 1 day (24–34 h) [...] lating [...] g a dissecting scope to count the number of protrusions from each o[...]oid. For Msi-1$^{-/-}$ and Msi-1$^{+/+}$ cultures, all organoids in all wells were scored for protrusions – 10–662 organoids in Msi-1$^{-/-}$ cultures [...]5 in Msi-1$^{+/+}$ cultures. Significance was calculated from cultures [...]ared [...] one mouse per genotype using a Student's t-test.

In situ hybridization

Lgr5 mRNA transcripts were detected on paraformaldehyde (PFA)-fixed, [...]araffin-embedded sections from wild-type and Msi-1-knockout mice using the [...]Ascope 2.5 Assay according to the manufacturer's instructions (cat. ACD-322350, Advanced Cell Diagnostics, Hayward, CA) and with probes for mouse Lgr5 (cat. no. ACD-312171), mouse PPIB (positive control, cat. no. ACD-313902) and DapB (negative control, cat. no. ACD-310043). After the Fast Red reaction, the slides were counterstained using hematoxylin and permanently mounted using Pertex® mounting medium. At least 20 crypts with at least one Lgr5-positive cell were scored for each mouse. Significance was calculated using a Student's t-test and results from at least eight mice of each genotype.

Supplementary information

Supplementary information available online at
http://jcs.biologists.org/lookup/doi/10.1242/jcs.197574.supplemental

References

Arumugam, K., MacNicol, M. C. and MacNicol, A. M. (2012). Autoregulation of Musashi1 mRNA translation during Xenopus oocyte maturation. *Mol. Reprod. Dev.* **79**, 553-563.

Barker, N., van Es, J. H., Kuipers, J., Kujala, P., van den Born, M., Cozijnsen, M., Haegebarth, A., Korving, J., Begthel, H., Peters, P. J. et al. (2007). Identification of stem cells in small intestine and colon by marker gene Lgr5. *Nature* **449**, 1003-1007.

Cambuli, F. M., Correa, B. R., Rezza, A., Burns, S. C., Qiao, M., Uren, P. J., Kress, E., Boussouar, A., Galante, P. A. F., Penalva, L. O. F. et al. (2015). A mouse model of targeted Musashi1 expression in whole intestinal epithelium suggests regulatory roles in cell cycle and stemness. *Stem Cells* **33**, 3621-3634.

de Sousa Abreu, R., Sanchez-Diaz, P. C., Vogel, C., Burns, S. C., Ko, D., Burton, T. L., Vo, D. T., Chennasamudaram, S., Le, S.-Y., Shapiro, B. A. et al. (2009). Genomic analyses of musashi1 downstream targets show a strong association with cancer-related processes. *J. Biol. Chem.* **284**, 12125-12135.

Gagliardi, G., Moroz, K. and Bellows, C. F. (2012). Immunolocalization of DCAMKL-1, a putative intestinal stem cell marker, in normal colonic tissue. *Pathol. Res. Practice* **208**, 475-479.

Gerbe, F., Brulin, B., Makrini, L., Legraverend, C. and Jay, P. (2009). DCAMKL-1 expression identifies Tuft cells rather than stem cells in the adult mouse intestinal epithelium. *Gastroenterology* **137**, 2179-2180; author reply 2180-2171.

Giannakis, M., Stappenbeck, T. S., Mills, J. C., Leip, D. G., Lovett, M., Clifton, S. W., Ippolito, J. E., Glasscock, J. I., Arumugam, M., Brent, M. R. et al. (2006). Molecular properties of adult mouse gastric and intestinal epithelial progenitors in their niches. *J. Biol. Chem.* **281**, 11292-11300.

Imai, T., Tokunaga, A., Yoshida, T., Hashimoto, M., Mikoshiba, K., Weinmaster, G., Nakafuku, M. and Okano, H. (2001). The neural RNA-binding protein Musashi1 translationally regulates mammalian numb gene expression by interacting with its mRNA. *Mol. Cell. Biol.* **21**, 3888-3900.

Itzkovitz, S., Lyubimova, A., Blat, I. C., Maynard, M., van Es, J., Lees, J., Jacks, T., Clevers, H. and van Oudenaarden, A. (2012). Single-molecule transcript counting of stem-cell markers in the mouse intestine. *Nat. Cell Biol.* **1**

Kawahara, H., Imai, T., Imataka, H., Tsujimoto, M., Matsumoto, K. and ano, H. (2008). Neural RNA-binding protein Musashi1 inhibits translation initia tion by competing with eIF4G for PABP. *J. Cell Biol.* **181**, 639-653.

Kayahara, T., Sawada, M., Takaishi, S., Fukui, H., Seno, H., Fukuzawa, Suzuki, K., Hiai, H., Kageyama, R., Okano, H. et al. (2003). Candidate mark for stem and early progenitor cells, Musashi-1 and Hes1, ssed in cryp base columnar cells of mouse small intestine. *FEBS Le 35*, 35.

Lamlum, H., Ilyas, M., Rowan, A., Clark, S., Johnso , Bell, J rayling, I., Efstathiou, J., Pack, K., Payne, S. et al. (1999). Th pe of soma mutation at APC in familial adenomatous polyposis is determ d by the site mutation: a new facet to Knudson's 'two-hit' hyp sis. *Nat. M* , 1071-1075.

Lan, L., Appelman, C., Smith, A. R., Yu, J., Larse Marq , R. T., Liu, H., Wu, X., Gao, P., Roy, A. et al. (2015). Natu product pol inhibits colon cancer cell growth by targeting RNA-bin g protein Mus . *Mol. Oncol.* **9**, 1406-1420.

Lewis, A., Segditsas, S., Deherago M., Pollard, P., Jeffery, Nye, E., Lockstone, H., Davis, H., Clark, S G. et al. (2010). Severe polyposis in Apc(1322T) mice is associated subma Wnt signalling and increased expression of the stem cell mar Lgr5. *Gut 59* -1686.

Li, N., Yousefi, M., Nakauka-Ddamba, A., Li, F., Va L., Parada, K., Woo, D.-H., Wang, S., Naqvi, A. S ao, S. et al. (2015). The ily of RNA-binding proteins function redundan as intestinal oncoproteins. *Cell ep.* **13**, 2440-2455.

Mach, N., Berri, M., Esc ré, D., Chevaleyre, C., Lemonnier, G., Billon, Y., Lepage, P., Oswald, Doré, J., el-Gaillard, C. et al. (2014). Extensive expression differen along porci mall intestine evidenced by transcriptome sequencing. *PLoS IE* **9**, e885

MacNicol, M. C., Cra E. MacNicol, A. (2011). Context-dependent regulation of Musashi- mRNA transl n and cell cycle regulation. *Cell Cycle* **10**, 39-44.

Maria Camb Rezza, A., N J. Plateroti, M. (2013). Brief report: Musash GFP a new tool for tial isolation of the intestinal stem cell popul s. *Stem C s* **31**, 2273-2278

May, Riehl, T. E. nt, C., Sureban, S. M., Anant, S. and Houchen, C. W. (2). Identificati ve gastrointestinal stem cell and adenoma cell marke oublecortin and CaM kinase-like-1, following radiation injury and nop s polyposis coli/multiple intestinal neoplasia mice. *Stem Cells* **26**, 630

Munoz, J., S D. E., Schepers, A. G., van de Wetering, M., Koo, B. K., Itzkovitz, S., V ann, R., Kung, K. S., Koster, J., Radulescu, S. et al. (2012). The Lgr5 in al stem cell signature: robust expression of proposed quiescent '+' cell markers. *EMBO J.* **31**, 3079-3091.

Muto, J., Imai, T., Ogawa, D., Nishimoto, Y., Okada, Y., Mabuchi, Y., Kawase, T., Iwanami, A., Mischel, P. S., Saya, H. et al. (2012). RNA-binding protein Musashi1 modulates glioma cell growth through the po scriptional regulation of Notch and PI3 kinase/Akt signaling pathways 33431.

Nakamura, M., Okano, H., Blendy, J. A. and Mo i, C. (1994). shi, a neural RNA-binding protein required for Drosop adult external s ory organ development. *Neuron* **13**, 67-81.

Nishimura, S., Wakabayashi, N., Toyo Kashima, K. and M fuji, S. (2003). Expression of Musashi-1 in human l colon crypt cells: ossible stem cell marker of human colon epithelium. *Dig Sci.* **48**, 1523 9.

Ootani, A., Li, X., Sangiorgi, E., H Q. T., Ueno, oda, S., gihara, H., Fujimoto, K., Weissman, I. L., ecchi, M. R. et al. S ained in vitro intestinal epithelial culture withi Wnt-dependent stem cel *Nat. Med.* **15**, 701-706.

**Pollard, P., Deheragoda, M egditsas, S ewis, A., Rowan, A., Howarth, K., Willis, L., Nye, E., McCa Mandir et al. (2009) e Apc 1322T mouse develops severe polyposis ciate ith submaxi nuclear beta-catenin expression. *Gastroen ology 1* -2213.e13.

Potten, C. S., Boot Tudor, G. L th, D., B y, G., Hurley, P., Ashton, G., Clarke, R., Sa ibara, S.-I. and Ok 4 (2 3). Identification of a putative intestinal stem and early lineage marker, shi-1. *Differentiation* **71, 28-41.

Rezza, A., Ska he, C., Nadjar, J., Sama ut, J. and Plateroti, M. (2010). The overe ssion putative gut stem cell marker Musashi-1 induces tumorige s through W Notch activation. *J. Cell Sci.* **123**, 3256-3265.

Sakakibara, S.-I., Nakamura, shida, T., Shibata, S., Koike, M., Takano, H., Ueda, S., Uchiyama, Y., Noda, and Okano, H. (2002). RNA-binding protein Mus lly: roles for CNS stem c s and a subpopulation of ependymal cells r ed by targeted disruption and antisense ablation. *Proc. Natl. Acad. Sci. USA* , 15194-15199.

giorgi, E. and Cap hi, M. R. (2008). Bmi1 is expressed in vivo in intestinal stem cells. *Nat. Genet* 915-920.

nsom, O. J., Reed, K Hayes, A. J., Ireland, H., Brinkmann, H., Newton, P., Batlle, E., Simon- smann, P., Clevers, H., Nathke, I. S. et al. (2004). Loss c in vivo immedi y perturbs Wnt signaling, differentiation, and migration. *G Dev.* **18**, 13 90.

Sato, T., Snippert, H. J., van de Wetering, M., Barker, N., Stange, D. E., van Es, J. H., Abo, A., Kujala, P., Peters, P. J. et al. (2009). Single Lgr5 stem cells build crypt-villus structures in vitro without a mesenchymal niche. , 262-265.

S emake R., Moser, A. R. and Dove, W. F. (1995). N-ethyl-N-nitrosourea reatment of multiple intestinal neoplasia (Min) mice: age-related effects on the formation of intestinal adenomas, cystic crypts, and epidermoid cysts. *Cancer Res.* **55**, 4479-4485.

Smith, A. R., Marquez, R. T., Tsao, W.-C., Pathak, S., Roy, A., Ping, J., Wilkerson, B., Lan, L., Meng, W., Neufeld, K. L. et al. (2015). Tumor suppressive microRNA-137 negatively regulates Musashi-1 and colorectal cancer progression. *Oncotarget* **6**, 12558-12573.

Spears, E. and Neufeld, K. L. (2011). Novel double-negative feedback loop between adenomatous polyposis coli and Musashi1 in colon epithelia. *J. Biol. Chem.* **286**, 4946-4950.

Stappenbeck, T. S., Wong, M. H., Saam, J. R., Mysorekar, I. U. and Gordon, J. I. (1998). Notes from some crypt watchers: regulation of renewal in the mouse intestinal epithelium. *Curr. Opin. Cell Biol.* **10**, 702-709.

Sureban, S. M., May, R., George, R. J., Dieckgraefe, B. K., McLeod, H. L., Ramalingam, S., Bishnupuri, K. S., Natarajan, G., Anant, S. and Houchen, C. W. (2008). Knockdown of RNA binding protein musashi-1 leads to tumor regression in vivo. *Gastroenterology* **134**, 1448-1458.e2.

Takahashi, T., Suzuki, H., Imai, T., Shibata, S., Tabuchi, Y., Tsuchimoto, K., Okano, H. and Hibi, T. (2013). Musashi-1 post-transcriptionally enhances phosphotyrosine-binding domain-containing m-Numb protein expression in regenerating gastric mucosa. *PLoS ONE* **8**, e53540.

VanDussen, K. L., Carulli, A. J., Keeley, T. M., Patel, S. R., Puthoff, B. J., Magness, S. T., Tran, I. T., Maillard, I., Siebel, C., Kolterud, A. et al. (2012). Notch signaling modulates proliferation and differentiation of intestinal crypt base columnar stem cells. *Development* **139**, 488-497.

Vogelstein, B., Fearon, E. R., Kern, S. E., Hamilton, S. R., Preisinger, A. C., Nakamura, Y. and White, R. (1989). Allelotype of colorectal carcinomas. *Science* **244**, 207-211.

Wang, Y., Azuma, Y., Friedman, D. B., Coffey, R. J. and Neufeld, K. L. (2009). Novel association of APC with intermediate filaments identified using a new versatile APC antibody. *BMC Cell Biol.* **10**, 75.

Zeineldin, M. and Neufeld, K. (2012). Isolation of epithelial cells from mouse gastrointestinal tract for western blot or RNA analysis. *Bio-protocol* **2**, e292.

Zeineldin, M. and Neufeld, K. L. (2013). Understanding phenotypic variation in rodent models with germline Apc mutations. *Cancer Res.* **73**, 2389-2399.

Zeineldin, M., Cunningham, J., McGuinness, W., Alltizer, P., Cowley, B., Blanchat, B., Xu, W., Pinson, D. and Neufeld, K. L. (2012). A knock-in mouse model reveals roles for nuclear Apc in cell proliferation, Wnt signal inhibition and tumor suppression. *Oncogene* **31**, 2423-237.
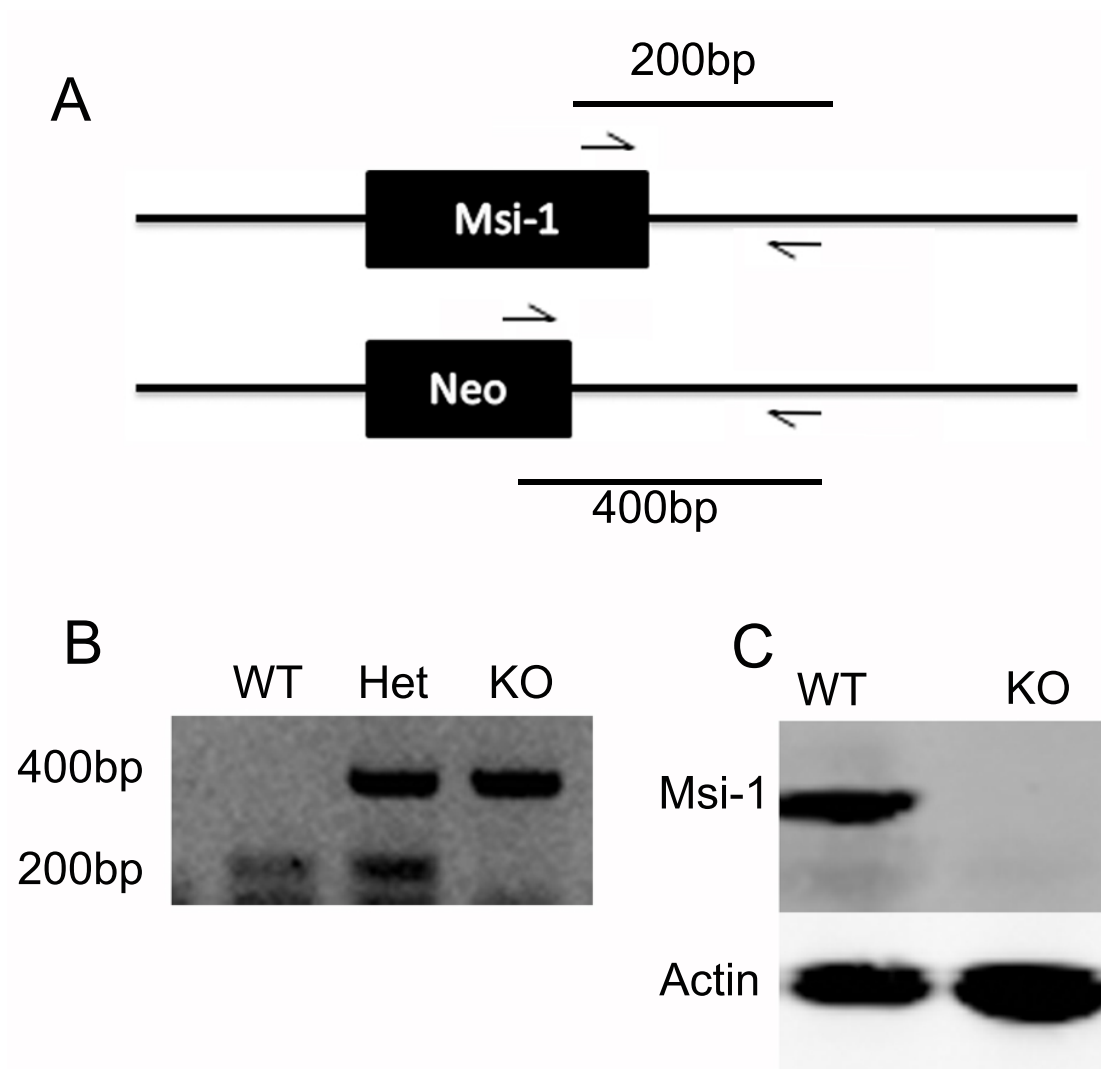
Fig. S1 **Validation of Msi-1 knock out mice.** (A) Msi-1$^{-/-}$ mice have a Neo^R cassette replacing the *Msi-1* gene. Primers were designed with a common reverse primer downstream of the gene and forward primers within either the *Msi-1* gene or the Neo cassette. (B) Representative image of PCR *Msi-1* genotyping results, WT=wild-type, Het=Msi-1 heterozygous, KO=Msi-1 knockout. (C) Immuno-blot of intestinal whole cell protein lysates probed for Msi-1 and actin (loading control).
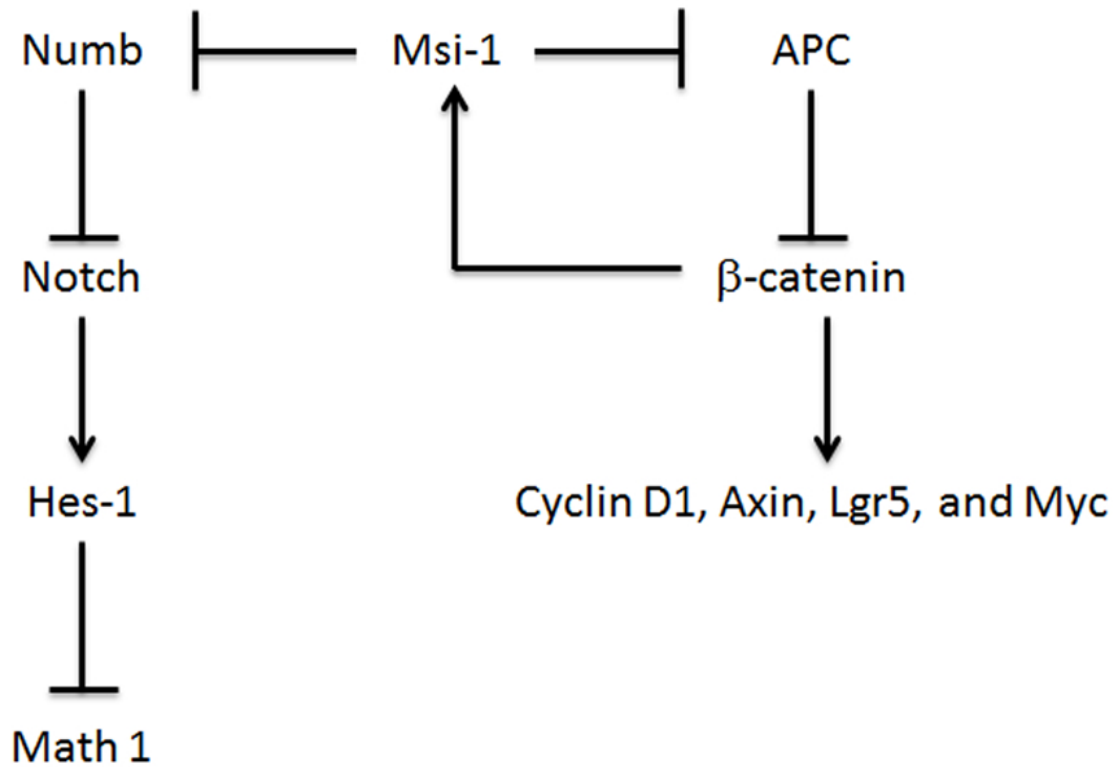
Fig. S2 **Msi-1 signaling networks interrogated in this study.** A simplified diagram of the Notch and Wnt Signaling pathways downstream of Msi-1 including the double negative feedback loop with APC.